Methods of Deterministic Chaos Applied to the Flow of Thin Wavy Films

C. E. Lacy, M. Sheintuch, and A. E. Dukler
Dept. of Chemical Engineering, University of Houston, Houston, TX 77204

The structure of thin, wavy falling films was studied to evaluate whether the random-appearing wave structure is a result of deterministic chaos or a purely stochastic process. The time-varying film thickness was obtained at different spatial locations near the point of wave inception for flow rates in the range of Re = 3–10. Under all conditions the wave structure was aperiodic in nature and displayed none of the known transitions to chaos. However, the power spectra followed an exponential decay law at high frequencies that is characteristic of chaotic systems. The estimated attractor dimension, used to characterize the complexity of a chaotic system, was much higher than those of known model chaotic systems. It is demonstrated that these high values could be explained due to small levels of noise present in experimental situations. Since experimental data are seldom noise free, a basic limitation in applying these methods to experimental measurements is demonstrated.

Introduction

The hydrodynamic behavior of thin wavy falling films has been a subject of intensive investigation for about forty years. These films are widely employed in equipment for heat transfer, mass transfer, and chemical reacting systems. In addition to the practical need for understanding the mechanics of this type of flow, there are challenging theoretical problems embedded in the task of modeling these wavy films. This combination has given rise to an extensive literature on this subject.

The earliest work was based on the use of integral equations of the boundary layer type to solve the equations of motion (Kapitza and Kapitza, 1949; Shkadov, 1967). These approaches were based on the assumed existence of a periodic interface and produced first-order estimates for wavelength and velocity. A long series of papers including work by Benney (1966), Lin (1969), and Whitaker (1964), used linear stability analysis to find the wavelength and velocity of the fastest growing wave, again assuming a periodic perturbation. This initial periodic disturbance is thought to evolve into the more complex waveforms observed in experiments as a result of the nonlinear nature of the equations. Nonlinear stability analyses have also been pursued (Pumir, 1983). Recent work on the nonlinear nature of wavy films (Chang, 1987; Sheintuch and Dukler, 1989) searched for infinitely long periodic waves by finding the conditions for existence of the homoclinic orbit.

But even a cursory examination of measured wave traces raises some doubts as to the usefulness of the idea of a small-amplitude periodic wave as the model for the initial phase of the wave motion or of isolated waves as a model for the developed ones. Figure 1d shows a wave trace for a falling liquid film of water–glycerine solution taken with a conductivity probe mounted in a vertical pipe of 50.8 mm dia. as described below. The flow rate corresponds to a Reynolds number of 3.9. The probe was located 0.346 m below a carefully leveled, sharp-edged overflow weir that served as the feed device. The film thickness data are shown after low-pass digital filtering at 25 Hz to remove noise. At this location the wave amplitude is less than 0.25% of the mean film thickness. At all positions closer to the feed the waves were so small that they could barely be detected even with the special circuitry used for this purpose. Note that while the period between successive waves is quite regular, the amplitude is very random. Kapitza and Kapitza (1949) in their classical study of waves on falling films found it necessary to pulse the feed to produce periodic waves. In the absence of pulsing they too reported that the waves were random in appearance. Thus one must question whether the

The present address of M. Sheintuch is Chemical Engineering, The Technion, Haifa, Israel.

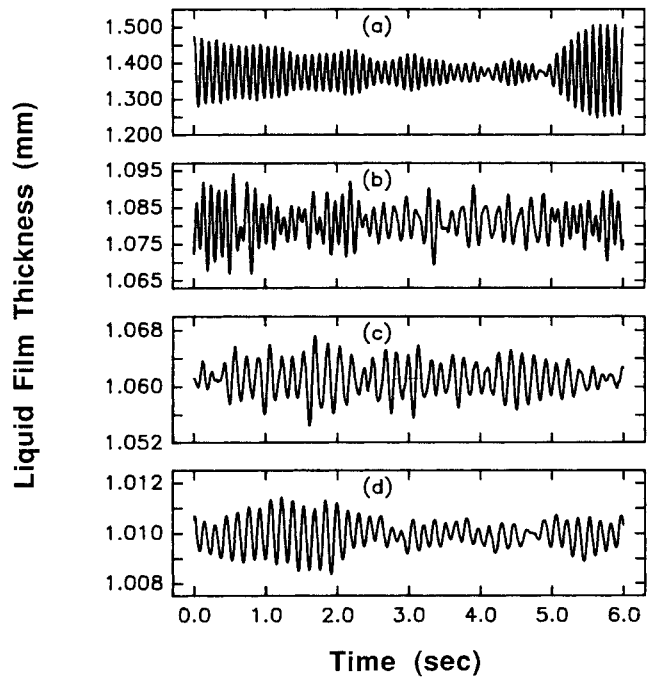

Figure 1. Experimental film thickness traces of low *Re* flow near wave inception point.

a. $Re=7.5$, probe 1 c. $Re=4.7$, probe 2
b. $Re=5.6$, probe 1 d. $Re=3.9$, probe 3

wave structure in the earliest phases of formation can be described as regularly periodic.

Figure 2 shows the wave trace for a much higher flow rate taken at a position 1.7 m below the feed and thus much farther down along the vertical surface. Now there are large variations in the distance between peaks as well as in the amplitudes of the waves. It seems difficult to picture this surface as being made up of a series of isolated waves that arise from homoclinic orbits.

In view of the omnipresent nature of the randomness, it would appear necessary to address the following questions if one is to hope to model the wave motion on these films.

1. Does the observed randomness in wave amplitude and period originate in microscopically small stochastic variations in feed rate or equipment vibrations, or is it a result of deterministic chaos? If the former is true then it will be necessary to find the stochastic forcing functions, suitably incorporate them into the equations of motion, and solve these complex nonlinear stochastic differential equations. If the appearance

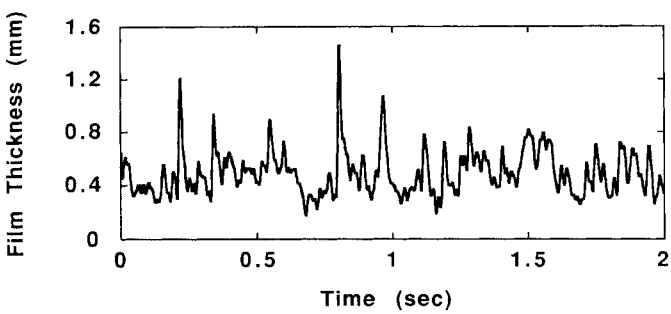

Figure 2. Film thickness time trace of a free-falling film.

$Re=1{,}550$, 1.7 m vertically below feed entry point

is a manifestation of deterministic chaos then it will be necessary to develop a set of model equations that display this behavior. Shivashinsky and Michelson (1980) have shown this type of behavior for a set of equations that resemble the shallow-water equation for free surface flows. However, their equations include only the lowest possible level of nonlinearity and do not model thin film wavy flows.

2. If this system is one displaying deterministic chaos, then it is of interest to estimate the attractor dimension since this provides some indication of the minimum number of ordinary differential equations needed to model the system, thus suggesting a lower limit to the degree of numerical approximation needed to solve the Navier-Stokes equations.

3. All existing models for chaos visualize a transition from an initial steady state to a periodic one and then to a chaotic condition by one of several possible paths. It is also of interest to determine whether this wavy film system obeys any of these transition mechanisms.

We approach these questions by attempting to analyze experimental data on the time-varying film thickness. In the course of doing so problems associated with treating experimental data accompanied by noise must be faced, and we report on this issue as well.

Method

The concept of attractor dimension has been widely used to distinguish between systems that are random and those that display deterministic chaos. (Brandstater and Swinney, 1987; Farmer, et al. 1983; Grassberger and Procaccia, 1983). Consider a chaotic system described by three first-order ordinary differential equations (ODE). When the solution is plotted in phase space with the coordinates as the three dependent variables of the system, the solution remains in a closed, bounded region of the phase space known as an attractor. When the motion is periodic the attractor is a line and thus its dimension is one. Quasiperiodic motion made up of two nonharmonic frequencies will form a two-dimensional torus. If the process is one displaying deterministic chaos, the attractor dimension falls between 2 and 3. On the other hand, if the process is statistically random, then the attractor will fill the entire phase space and its dimension will be 3. This reasoning can now be extended to any D-dimensional phase space formed by D first-order differential equations. Periodic and quasiperiodic processes display dimensions of 1 and 2; the dimension of a chaotic process will fall between 2 and D, and a random process has an attractor of dimension D.

In order to estimate the attractor dimension from experimental data when model equations do not exist, it is necessary to reconstruct the phase space. A phase space having the same topological properties as the true phase space can be constructed from a time series by using time-delayed copies (Berge et al. 1984). For example, an attractor in the D-dimensional phase space can be constructed from a digitized time series by forming a sequence of D-dimensional vectors, x_i, by

$$x_i=[x(t_i),\ x(t_i+\tau),\ x(t_i+2\tau),\ \ldots\ ,\ x(t_i+(D-1)\tau)] \quad (1)$$

Criteria for selecting the delay time, τ, are discussed below. If an attractor exists in the actual phase space, its dimension can be approximated by applying one of several scaling laws

to the reconstructed phase space, since the reconstructed and actual phase space have the same topological properties. If the system is one characterized by deterministic chaos, then its dimension, d, is independent of D. It has been shown by Takens (1981) that $D>2d+1$ is necessary to obtain a good estimate of d.

In this study the nearest-neighbor method of Badii and Politi (1985) was used to estimate the dimension since it appears to be more accurate (Kostelich and Swinney, 1987) than the more widely used correlation dimension method of Grassberger and Proccaccia, (1983) for systems displaying higher dimensions. Consider a set of N points, constructed as in Eq. 1, that lie on the reconstructed attractor. Arbitrarily select a point $\boldsymbol{x}$ on this attractor as a reference point. Now choose at random a subset of k points denoted by $y_i (i=1,2,\ldots,k$ and $k<N)$ from the original set of N points and consider the distance from $\boldsymbol{x}$ to each point y_i. Define δ as the single minimum of these distances, that is, the distance to the nearest neighbor.

$$\delta = \min \|\boldsymbol{x} - y_i\| \tag{2}$$

To obtain a statistically useful value of the minimum distance, this calculation is repeated over many randomly chosen reference points and an average obtained, $\langle\delta\rangle$. The process is then repeated for a sequence of k values up to $k=N-1$ for each $\boldsymbol{x}$. The number of nearest neighbors contained in a D-dimensional hypersphere of radius δ around a given point should vary as δ^d if the attractor is d-dimensional. Thus it is argued that

$$\langle\delta\rangle \sim k^{(-1/d)} \tag{3}$$

Hence

$$\log\langle\delta\rangle \sim \frac{-1}{d} \log k \tag{4}$$

The negative, inverse slope of a log $\langle\delta\rangle$ vs. log k plot is the fractal dimension.

All experimental measurements of forced flow systems include electronic noise as well as noise due to random vibrations reaching the system through piping or pumps. Small-amplitude noise can be expected to distort distances between closest nearest neighbors and their reference point. To partly alleviate this error Kostelich and Swinney (1987) suggest that δ be calculated for the tenth or hundredth nearest neighbor. For each choice of D and nearest neighbor, n, an estimate of d can be calculated assuming k is kept sufficiently larger than n. The value of d is said to converge to the attractor dimension when d becomes independent of D and n as both are increased. Additional aspects of the noise problem are discussed later in this paper.

The computed value of d has been shown to depend on the value of the delay time, τ, used to construct the D-dimensional vectors in Eq. 1. If τ is too small, then each $x(t)$ approaches $x(t+\tau)$, and the reconstructed attractor will be a 45° plane in the phase space. For large values of τ, the attractor dimension tends to approach the embedding dimension, D, of the reconstructed phase space due to the stretching and folding nature of chaotic systems (Fraser and Swinney, 1986).

To obtain the optimal delay, a series of two-dimensional reconstructions of $\{x(t), x(t+\tau)\}$ are generated with increasing values of τ. The optimal reconstruction occurs for the smallest value of τ for which $x(t)$ and $x(t+\tau)$ can first be considered independent. The criterion for choosing this value of τ is the first minimum in the index of mutual information, I, as described by Fraser and Swinney (1986). This index is a measure of the degree of predictability of a measurement $x(t+\tau)$ given a measurement $x(t)$.

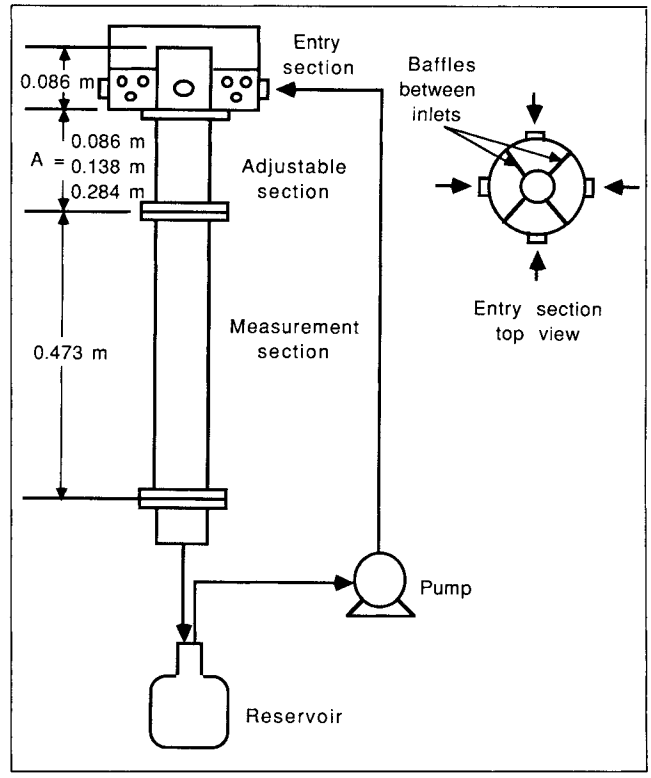

Figure 3. Low *Re* flow system.

Experimental Equipment

Figure 3 is a diagram of the experimental flow loop used for studies of free-falling liquid films at low $Re (Re=4Q/v = 3\text{–}10)$. Where Q is the volumetric flow rate per unit perimeter and v is the kinematic viscosity. The measurement section consisted of a 50.8 mm dia. tube 0.47 m long. The liquid feed tank contained a sharp-edged circular weir over which the liquid flowed from the reservoir into the pipe. The distance from the sharp edge to the bottom of the flange was 86 mm. This was followed by a development section having one of three lengths: 86, 138, or 284 mm. Wave motion is not observed immediately after the film is formed at the overflow. The development section provided the length needed at different flow rates to cause the waves to first appear in the measuring section where film thickness probes were located.

Instantaneous film thickness data were obtained using closely spaced parallel wires to make resistivity measurements, which are related to film thickness by calibration. Details of this method including the electronic circuit used appear in the thesis by Zabaras (1985). For these low Re measurements, an array of seven probes was spaced in the direction of flow with distances from the feed point listed in Table 1. A glycerine-water-NaOH solution having a kinematic viscosity of 5.6×10^{-5}

Table 1. Low Reynolds No. Film Thickness Measurements

Reynolds No., *Re*	Probe No.	Filter Cutoff Freq. Hz	Dist. from Feed cm	Time Delay Points
9.2	3	no filter	16.9	5
	4	no filter	21.9	5
	5	no filter	31.9	8
	6	no filter	41.9	8
7.5	1	no filter	20.8	6
	2	no filter	22.5	6
	3	no filter	25.5	6
	4	no filter	30.5	6
	5	no filter	40.5	7
	6	no filter	50.5	7
	7	no filter	60.5	7
5.6	1	60	26.0	8
	2	60	27.7	7
	3	120	30.7	7
	4	120	35.7	8
	5	120	45.7	9
	6	120	55.7	10
	7	120	65.7	8
4.7	2	40	27.7	11
	3	40	30.7	12
	4	60	35.7	10
	5	60	45.7	10
	6	120	55.7	9
	7	120	65.7	10
3.9	3	25*	34.6	10
	4	60	44.3	10
	5	120	54.3	10
	6	120	64.3	10
	7	120	74.3	10

*Digital filtering

m^2/s at 25°C was used as the conducting fluid. The data were low-pass filtered to eliminate electronic noise and digitized at 250 Hz. Power spectral densities were calculated for 64 traces of 1,024 points each, thus producing a frequency resolution of about 0.25 Hz and estimated standard mean error of any spectral value of 12.5%.

Film thickness data for higher Reynolds numbers (310–3,100) were available from measurements in a vertical tube of the same diameter taken earlier in this laboratory (Zabaras and Dukler, 1988). These measurements included information for free-falling films, for counterflow of liquid and gas with the liquid flowing down, as well as for upward concurrent flow of the phases. Water and air were the fluids for this earlier study with the data digitized at 500 Hz.

Results

Low Reynolds number flows

Time Traces and Spectra. Table 1 lists the conditions for five runs executed at low *Re* along with information on the low-pass filter frequency used to reduce noise and the time delay used to construct the attractor from the time series. The frequency indicated in column 3 is the frequency of a low-pass analog filter at which the power is attenuated by one-half.

Figure 1 shows film thickness traces for each *Re* for the position closest to the inlet weir at which waviness could first be detected for that flow rate. In this region the waves are observed to fall as a two-dimensional ring structure. The power

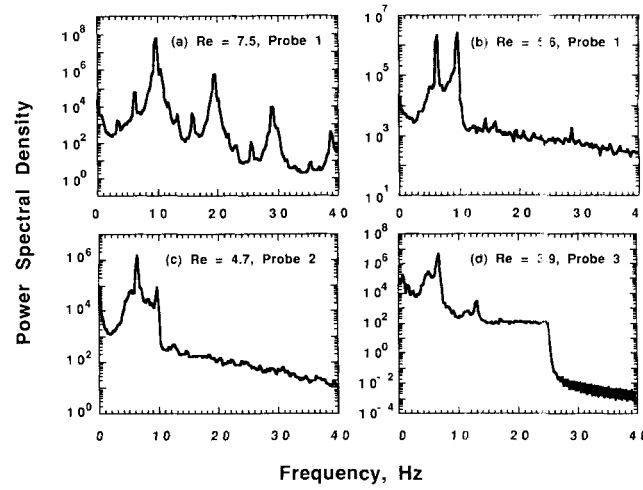

Figure 4. Power spectral density near wave inception point.

spectral density corresponding to these traces appears in Figure 4. For $Re < 5.6$, the spectra show a dominant frequency of 6.2 Hz while at $Re > 5.6$ the dominant frequency is 9.8 Hz. $Re = 5.6$ appears to be a transitional flow with the power spectrum displaying these two nonharmonic frequencies at almost equal power.

Since these data were taken at conditions close to the point of wave initiation where the amplitudes were small relative to the mean film thickness, it is of interest to compare the measured dominant frequencies with those predicted from linear stability theory for the fastest growing wave.

Re	3.8	4.7	5.6	7.5
f_{dm}	6.2	6.2	6.2,9.8	9.8
f_{dp}	7.1	8.0	8.7	9.9

f_{dm} is the measured dominant frequency while f_{dt} is the predicted value. Agreement is lacking and the transition from the flat film steady state to a Hopf bifurcation does not seem to exist. The data show chaotic character without having passed through a Hopf bifurcation, a process of period doubling, or any of the other mechanisms for transition to chaos that have been described in the literature.

Changes in the nature of the wave motion can be observed visually as they travel downward. The ring-type structure distorts, with some portions of the ring moving downward more rapidly in the form of fingers into the wave structure below. $Re = 7.5$ is typical of the case where only one dominant frequency exists at the plane of wave inception while $Re = 5.6$ shows two nearly equal frequencies at inception. Figure 5 shows how the wave traces at $Re = 7.5$ change at four locations from the entry weir ranging from 0.21 to 0.61 m below the overflow weir. The corresponding spectra and phase plane plots appear in Figures 6 and 7. Time delays used in Figure 7 are listed in Table 1. The spectral character stays basically unchanged with measurement location in the axial direction until the lowest position is reached. The phase planes show that close to inception the waves display regular periodicity with irregular amplitudes. At $Re = 7.5$ as they propagate downward this irregularity diminishes and the waves begin to approach a periodic state. Before uniformity in amplitude can be reached the wave acquires some features of the soliton, with the trough

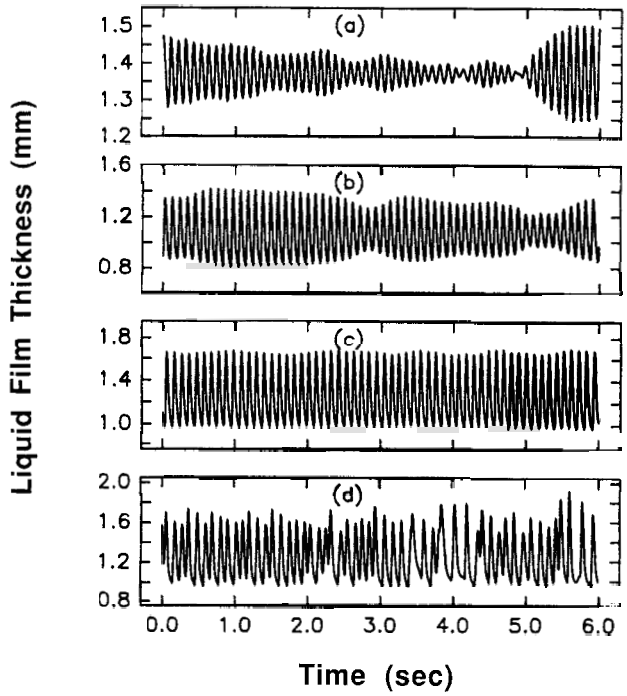

Figure 5. Experimental film thickness traces at $Re = 7.5$.

Distance below overflow weir:
a. 0.21 m; b. 0.26 m; c. 0.41 m; d. 0.61 m

of all the waves returning to a single thickness and the variation of wave amplitude being reflected in differences in the peak value. Figure 7c shows this structure in which the lefthand corner resembles motion in the vicinity of a saddle point. With further distance in the axial direction the wave periods, which heretofore had been regular, now become chaotic, as shown in the time trace, the spectrum, and in Figure 7d.

When two spectral peaks of about equal power exist at wave inception ($Re = 5.6$), the approach to a more uniform wave amplitude is not observed and the waves progress more rapidly to the condition of chaotic wave periods.

The power spectra provide a suggestion that the underlying process may be a manifestation of deterministic chaos. Sigeti and Horsthemke (1987) have shown that for a jth-order stochastic differential equation the spectral power at high frequencies follows a power law decay, $S = cf^{-2j}$. Deterministic equations are, on the other hand, infinitely differentiable and the spectrum must decay exponentially at high frequencies. All spectra observed were characterized by exponential decay.

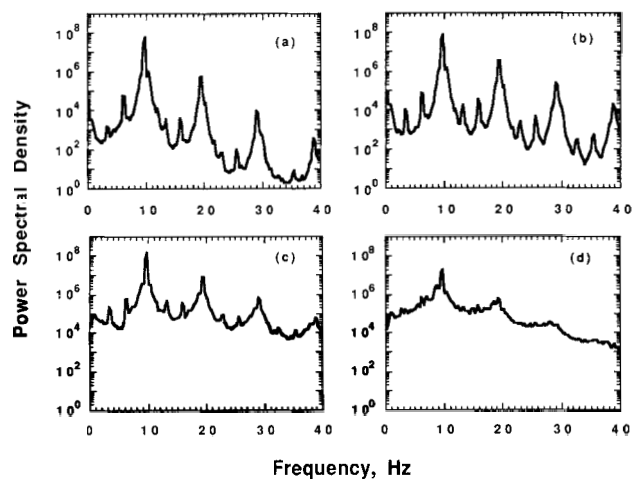

Figure 6. Power spectral density of $Re = 7.5$ data in Figure 5.

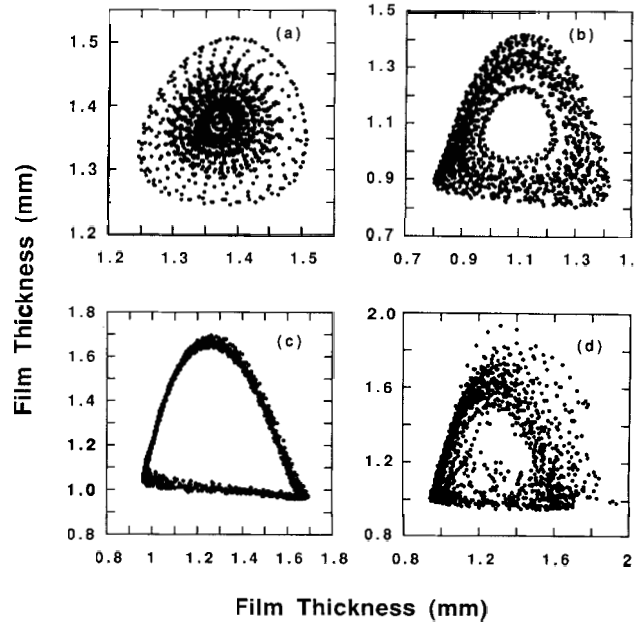

Figure 7. Phase plane portraits of $Re = 7.5$ data in Figure 5.

Attractor Dimension. For each data set listed in Table 1, the nearest-neighbor algorithm for the computation of the attractor dimension was applied using the following parameters:

Total points, N	=	100,000
Embedding dimension, D	=	8–20
Nearest neighbors, n	=	**100–600**
Subsets of N points, k	=	15,000–100,000

These parameters resulted in processing 2,000–4,000 waves with each wave represented by 30–40 discrete points.

Figure 8 illustrates the method of Badii and Politi (1985) when applied to the time series data from probe 5 at $Re = 7.5$. Figure 8a is a plot of $\log_2 \langle \delta \rangle$ vs. $\log_2 k$ for one D and n pair. An estimate of the attractor dimension, d, is obtained from the slope as given by Eq. 4. The results of repeating this process for each combination of D and n appear in Figure 8b. Here the dimension has converged with increasing D and n, indicating an attractor dimension of about 3.5. There are instances where convergence was not observed with increasing D, as illustrated in Figure 9, although convergence with increasing n was always observed. However, this system does not represent purely stochastic noise, since under that condition one would expect d to be close to D. This behavior seems to be related to the presence of noise in the signal and presents a basic problem in processing and analyzing data from real systems as compared to analyzing data from mathematical models.

Figure 10 shows the trends in complexity of the time traces as position and flow rates are changed. Estimated dimensions appear here that have been computed for $D = 20$, $N = 100{,}000$, $n = 600$ using 1,000 reference points. In some cases definitive

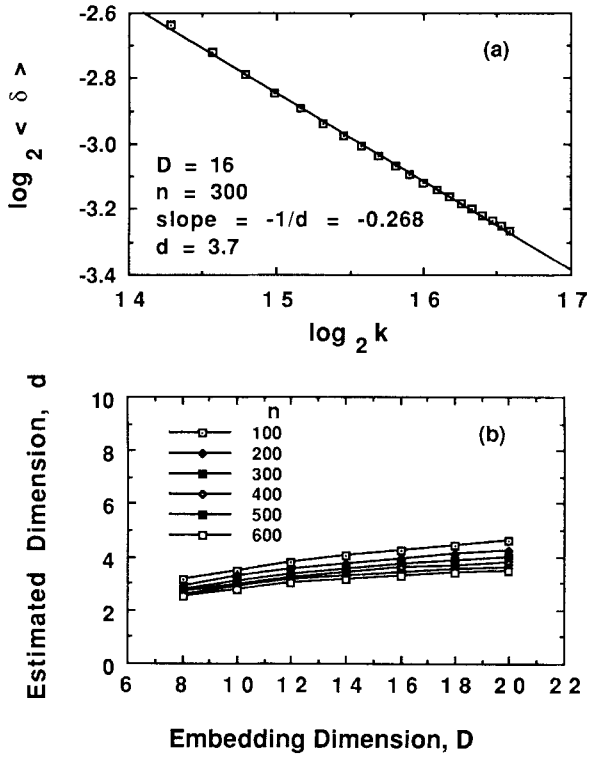

Figure 8. Calculation of attractor dimension for data at $Re = 7.5$, probe 5.

a. Determination of d from slope
b. Dependence of D and n on estimated dimension

convergence was not obtained. The data show an initial decline in the dimension as the flow rate is increased, followed by a sharp rise past the minimum. Except near the minima, the dimensions seem unreasonably high compared to model systems that have been studied, indicating the need to determine the role of noise in influencing the dimension of the attractor.

The Effect of Noise. As a practical matter, the requirement to analyze experimental data in contrast to data from mathematical models introduces the problem of the influence of noise on the computed results. To study this matter, several noisy signals were generated and their dimension measured. A sine wave, x, of unity amplitude was altered by the implementation of multiplicative or additive noise as follows:

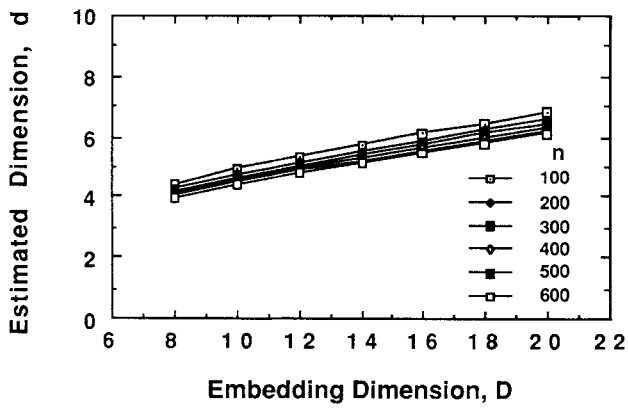

Figure 9. Illustration of no convergence in calculation of attractor dimension; $Re = 5.6$, probe 5.

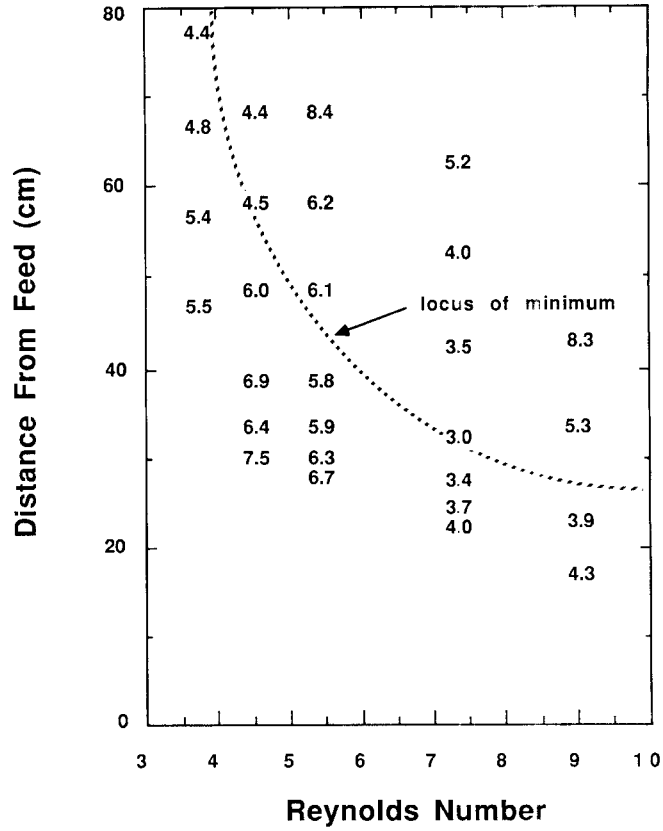

Figure 10. Estimated values of attractor dimension at $D = 20$, $n = 600$.

Multiplicative

$$x = \left[1 - z + z(v_{i+1} - v_i)\left(\frac{j}{L}\right) + zv_i\right]\sin\left(\frac{2\pi j}{j_o}\right)$$

Additive:

$$x = \sin\left(\frac{2\pi j}{j_o}\right) + zv(j)$$

The random noise component, v_i, was obtained from a uniformly distributed random number generator within the range $(-1,1)$ having an amplitude z. The value of j_o was chosen to be $\pi/0.14$ providing ~ 22 points per cycle, consistent with the analyses of the low Reynolds number data discussed above. L was arbitrarily chosen as 50. The effect of this process of noise addition was to alter the amplitude about every cycle for the multiplicative noise and every point for the additive noise.

Time traces are shown in Figures 11 and 12 for multiplicative and additive noise, respectively. The simulations shown for multiplicative noise strongly resemble the experimental measurements shown in Figure 1. For the sine wave without noise the computed dimension converged definitively to a value of 1.03. As can be seen from Figure 13, in the presence of even small amounts of multiplicative noise the dimension is substantially higher. For additive noise the distortion is even worse, as shown in Figure 14, where the degree of convergence becomes unsatisfactory.

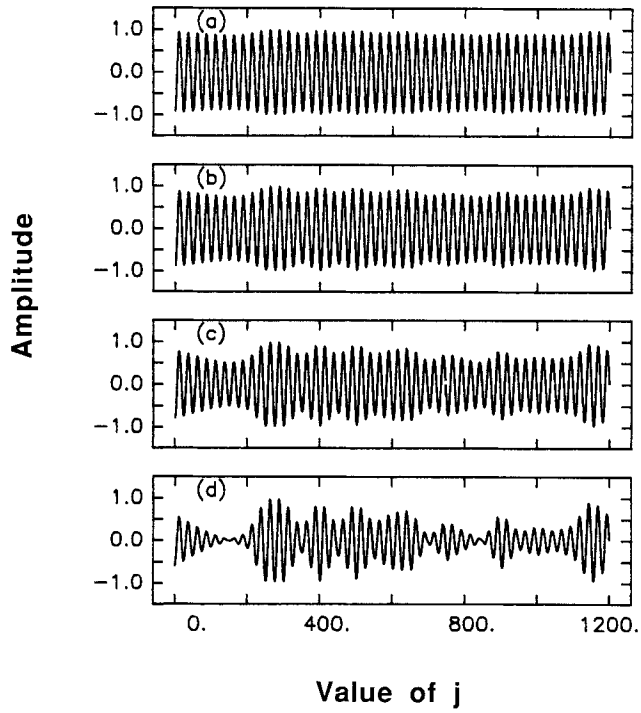

Figure 11. Time trace for a sine wave with multiplicative noise.

a. $z=0.125$; b. $z=0.25$
c. $z=0.5$; d. $z=1.0$

Attempts to diminish the effects of noise by low-pass filtering had negligible impact on the calculated dimension of the attractor. Methods for eliminating noise have recently been advanced by Kostelich and Yorke (1988), but they appear applicable only when the noise is small ($<1\%$), a condition that does not appear to exist here. Until improved methods are available, it would appear that this method for determining

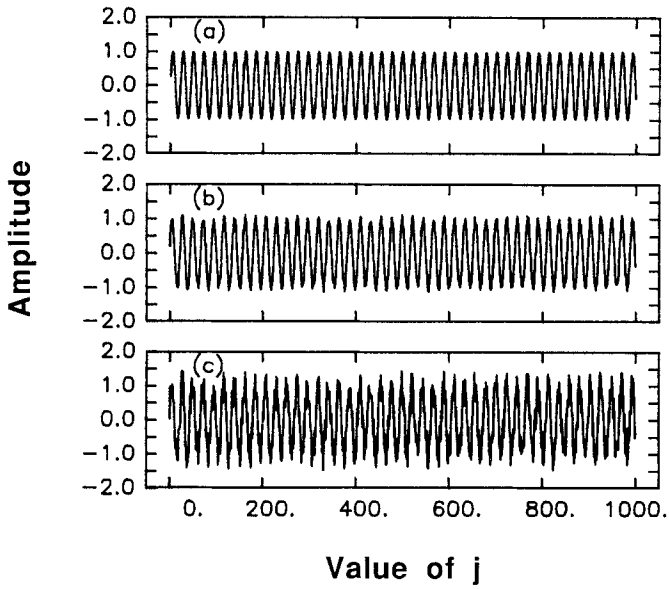

Figure 12. Time trace for a sine wave with additive noise.

a. $z=0.025$; b. $z=0.15$; c. $z=0.5$

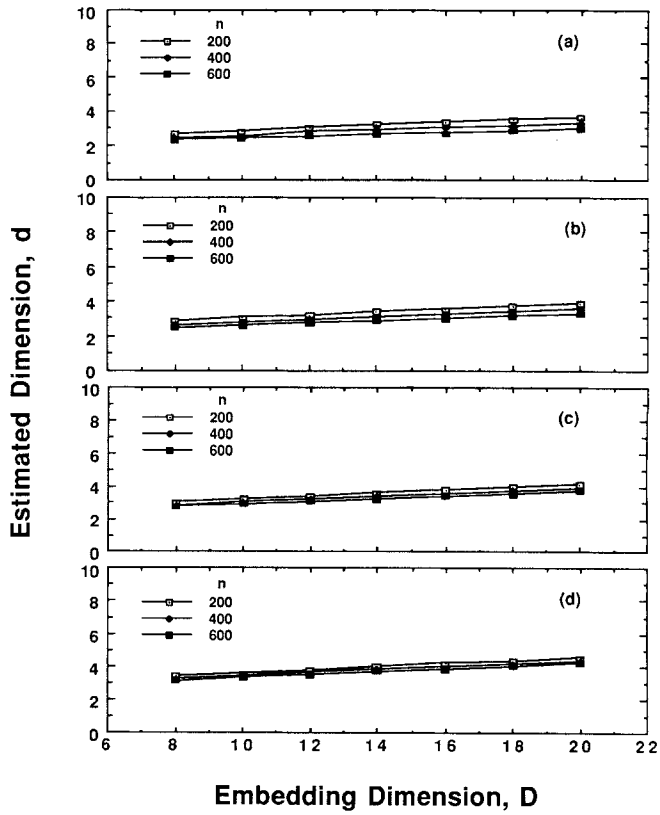

Figure 13. Dimension estimates for a sine wave with multiplicative noise.

a. $z=0.125$; b. $z=0.25$
c. $z=0.5$; d. $z=1.0$

if a process displays the characteristics of deterministic chaos will be of very limited utility when applied to experimental data from physical systems.

High Reynolds number flows

Figure 2 is representative of the time trace obtained at higher flow rates. The spectrum appears in Figure 15. Attractor dimensions were calculated for ten conditions in the range $Re=310$–$3{,}100$ and include data for free-falling films as well as those with countercurrent and cocurrent interfacial shear. All of these traces were characterized by poor convergence and high dimension. Extensive studies did not reveal any coherent dependence on Re or on the amount or direction of the interfacial shear. However, the high-frequency end of the spectrum still indicates an exponential decay, suggesting deterministic chaos. It is likely that noise plays a large role at these high rates where isolation of the system is more difficult.

Discussion

An extensive literature exists for analyzing time-dependent data using methods of fractal geometry. When the data are developed from mathematical models these methods of analysis provide new insights into the behavior of these nonlinear equations. However, attempts to analyze data obtained directly from experiment, as has been presented in this paper, face severe difficulties. Such data are accompanied by significant amounts of noise, and it is shown that noise levels commonly

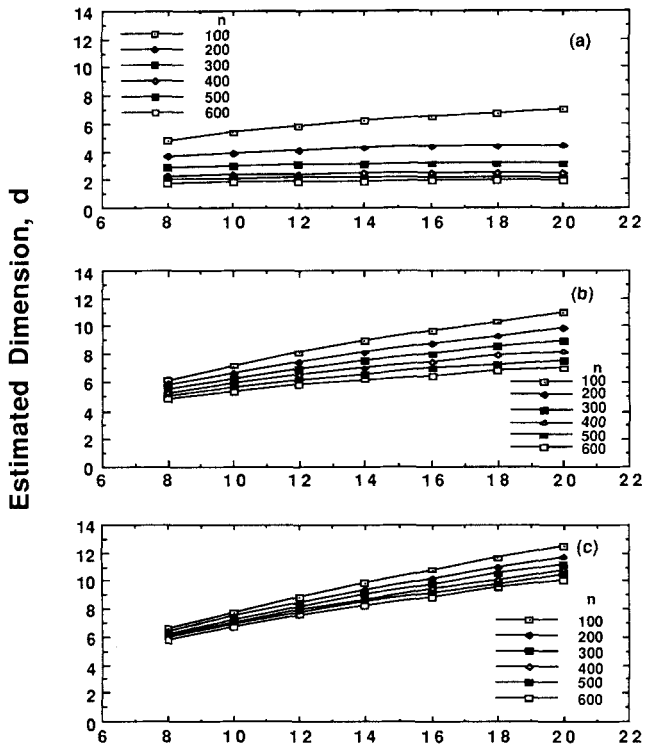

Figure 14. Dimension estimates for a sine wave with additive noise.

a. $z=0.025$; b. $z=0.15$; c. $z=0.5$

encountered in laboratory systems can seriously distort the results. Methods for suppressing the influence of noise have recently been proposed, but they are useful only when the noise represents less than a few percent of the signal. In open-flow systems this level can seldom be achieved.

The data presented in this paper show that even at very low Reynolds numbers in a carefully conducted experiment, falling liquid films are aperiodic. Near the condition of wave inception where the wave amplitudes are very small the measured frequencies are in poor agreement with the predictions of stability theory. Close to the position along the film where waves can first be detected, the presence of noise results in large values of the attractor dimension.

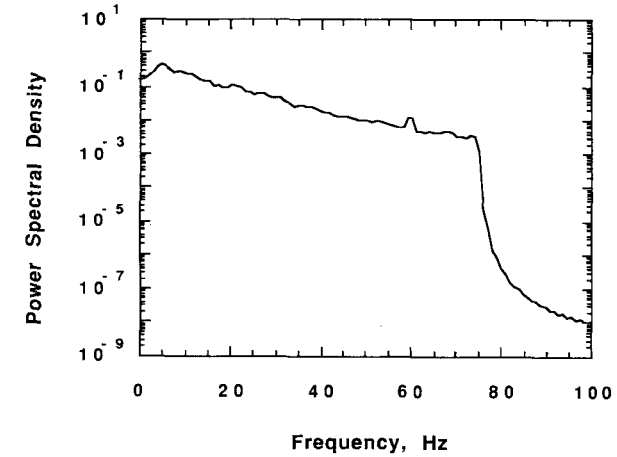

Figure 15. Power spectral density of a free-falling film.

$Re=1{,}550$, 1.7 m vertically below feed entry point
Digital low-pass filtering at 75 Hz

As the wave grows the relative importance of the noise decreases and the dimension decreases. Then with increasing distance along the film the waves distort and the dimension again becomes high. One never observes a sequence of transitions from the steady state flat film to periodicity and then to chaos. There is no evidence of frequency doubling. Even when the waves are of very small amplitude near their origin they appear chaotic. This is exactly the condition at which one would expect low-order deterministic chaos to characterize the behavior. However this study shows that existing methods of analysis do not. Before these methods can be of general use in analyzing data from physical experiments, new and improved noise elimination methods are needed.

Acknowledgment

The authors thank Eric Kostelich and Harry Swinney at the University of Texas for the use of their Cray Fortran code to perform the nearest-neighbor calculations. This work was supported by the National Aeronautics and Space Administration, Grant No. NAG-3-510 and its Graduate Student Researchers Program, Grant Nos. 88-026, 89-017, and 90-010.

Notation

c = a constant
d = actual or estimated attractor dimension
D = imbedding dimension
f = frequency
k = subset of N points
I = index of mutual information
n = order of nearest neighbor
N = total number of points
Q = volumetric flow rate per unit perimeter
S = spectral power
t = time
v = uniformly distributed noise $(-1,1)$
x = time series
$\mathbf{x}$ = vector of time series of dimension D
$\mathbf{y}$ = vector of time series of dimension D
z = fraction of signal due to noise

Greek letters

δ = nearest neighbor distance
ν = kinematic viscosity
τ = time delay

Literature Cited

Badii, R., and A. Politi, "Statistical Description of Chaotic Attractors: The Dimension Function," *J. Stat. Phys.*, **40**(5/6), 725, (1985).

Benney, D. J., "Long Waves on Liquid Films," *J. Math Phys.*, **45**, 150, (1966).

Berge, P., Y. Pomeau, and C. Vidal, *Order Within Chaos: Towards a Deterministic Approach to Turbulence*, Wiley, New York (1984).

Brandstater, A., and H. L. Swinney, "Strange Attractors in Weakly Turbulent Couette-Taylor Flow," *Phys. Rev. A.*, **35**(5), 2207 (1987).

Chang, H.-C., "Evolution of Nonlinear Waves on Vertically Falling Films—A Normal Form Analysis," *Chem. Eng. Sci.*, **42**, 515 (1987).

Farmer, J. D., E. Ott, and J. A. Yorke, "The Dimension of Chaotic Attractors," *Physica*, **7D**, 153 (1983).

Fraser, A. M., and H. L. Swinney, "Independent Coordinates for Strange Attractors from Mutual Information," *Phys. Rev. A.*, **33**(2), 1134 (1986).

Grassberger, P., and I. Procaccia, "Measuring the Strangeness of Strange Attractors," *Physica*, **9D**, 189 (1983).
Kapitza, P. L., and S. P. Kapitza, "Wave Flow of Thin Layers of a Viscous Fluid," *Zh. Exper. i Teor Fiz.*, **19**, 105 (1949); also in *Coll. Papers of P. L. Kapitza*, Macmillan, New York (1964).
Kostelich, E. J., and H. L. Swinney, "Practical Considerations in Estimating Dimension from Times Series Data," *Chaos and Related Nonlinear Phenomena*, Plenum, New York (1987).
Kostelich, E. J., and J. A. Yorke, "Noise Reduction in Dynamical Systems," *Phys. Rev. A.*, **38**(3), 1649, (1988).
Lin, S. P., "Finite Amplitude Stability of Parallel Flow with a Free Surface," *J. Fluid Mech.*, **36**, 113, (1969).
Pumir, A., P. Manneville, and Y. Pomeau, "On Solitary Waves Running Down an Inclined Plane," *J. Fluid Mech.*, **135**, 27 (1983).
Sheintuch, M., and A. E. Dukler, "Phase Plane and Bifurcation Analysis of Thin Wavy Films Under Shear," *AIChE J.*, **35**(2), 177 (1989).
Shkadov, V. Y., "Wave Flow Regimes of a Thin Layer of Viscous Fluid Subject to Gravity," *Izv. Akad. Nauk. Ser. Cekh. Zhidk. i Gaza*, **1**, 43 (1967).
Sigeti, D., and W. Horsthemke, "High-Frequency Power Spectra for Systems Subject to Noise," *Phys. Rev. A.*, **35**(5), 2276, (1987).
Sivashinsky, G. I., and D. M. Michelson, "On the Irregular Wavy Flow of a Liquid Film Down a Vertical Plane," *Prog. Theor. Phys.*, **63**, 2112 (1980).
Takens, F., in *Dynamical Systems and Turbulence*, Lecture Notes in Mathematics, **898**, D. A. Rand, L. S. Young, eds., Springer, Berlin, 137 (1981).
Whitaker, S., "Effect of Surface Active Agents on the Stability of Falling Films," *Ind. Eng. Chem. Fundam.*, **3**, 132, (1964).
Zabaras, G. J., "Studies of Vertical Annular Gas–Liquid Flows," PhD Thesis, Univ. Houston (1985).
Zabaras, G. J., and A. E. Dukler, "Countercurrent Gas–Liquid Annular Flow, Including the Flooding State," *AIChE J.*, **34**(3), 389 (1988).

Manuscript received July 3, 1990, and revision received Jan. 23, 1991.